Biomaterials 32 (2011) 3303–3311

Contents lists available at ScienceDirect

Biomaterials

journal homepage: www.elsevier.com/locate/biomaterials

The structural orientation of antibody layers bound to engineered biosensor surfaces

Anton P. Le Brun [a,1], Stephen A. Holt [b,1], Deepan S.H. Shah [c], Charles F. Majkrzak [d], Jeremy H. Lakey [a,*]

[a] Institute for Cell and Molecular Biosciences, The Medical School, Newcastle University, Framlington Place, Newcastle upon Tyne NE2 4HH, United Kingdom
[b] ISIS Neutron Facility, STFC Rutherford Appleton Laboratory, Harwell Science and Innovation Campus, Didcot, Oxfordshire OX11 0QX, United Kingdom
[c] Orla Protein Technologies Ltd, Biosciences Centre, International Centre for Life, Times Square, Newcastle upon Tyne NE1 4EP, United Kingdom
[d] NIST Centre for Neutron Research, National Institute for Standards and Technology, Gaithersburg, MD 20899, USA

ARTICLE INFO

Article history:
Received 23 December 2010
Accepted 8 January 2011
Available online 7 February 2011

Keywords:
Magnetism
Protein
Surface analysis
Surface modification
Gold
Immunochemistry

ABSTRACT

This paper describes a membrane protein array that binds immunoglobulin G at its constant regions whilst leaving the variable regions free to bind antigen. The scaffold of the array is the transmembrane domain of outer membrane protein A (tOmpA) from *Escherichia coli* engineered to assemble as an oriented monolayer on gold surfaces *via* a single cysteine residue. Other protein domains can be fused to the N and C termini of the scaffold. In this study we use circularly permuted ctOmpA fused to two Z domains of *Staphylococcus aureus* protein A (ZZctOmpA) to create the immunoglobulin G-binding array. The solution structure of the engineered proteins was assessed by circular dichroism spectroscopy. Assembly of the array, attachment of antibodies and antigen binding were measured using surface plasmon resonance and neutron reflection. Compared to mouse IgG2, polyclonal IgG from rabbit bound very strongly to ZZctOmpA and the dissociation of the immunoglobulin was slow enough to allow neutron reflection studies of the assembled layer with antigen. Using both magnetic and isotopic contrasts a complete layer by layer model was defined which revealed that the 223 Å high layer contains antibodies in an upright orientation.

1. Introduction

The biosensor market is driven by the need to identify and/or quantify biomolecules in complex samples in a rapid, reliable and economic way. The molecular recognition step is provided by biological molecules in many guises including: proteins, nucleic acids or even microorganisms. Proteins such as enzymes, antibodies, ion channels and receptors are polymers that can have highly specific functions and affinities for analytes and make ideal materials for biosensors. The transducer that converts the recognition event to an output can take the form of a conductimetric [1], dielectrimetric [2], optical [3], colourimetric [4], acoustic [5] or surface plasmonic [6] measurement. The ideal output is an electrical signal presented on a digital display. However, the marriage of the sensing component of a biosensor to a transducer is one of the biggest technical challenges in biosensor development [7]. The biological component usually needs to be immobilised to a surface and the most commonly used test in medical diagnosis is the immunoassay, which uses specific antibodies to bind the target molecule. Our goal is to assemble, on transducer surfaces, antibodies at the highest possible density and correctly orientated for antigen binding.

We have previously described the formation of dense oriented monolayers on gold surfaces using outer membrane proteins from bacteria [8,9]. These can be engineered to display selected protein sequences in a highly ordered manner [10]. One such group of proteins are the antibody-binding domains from the surface of infectious bacteria such as *Staphylococcus* and *Streptococci* [11]. One protein in particular *Staphylococcus aureus* protein A (SpA) has five immunoglobulin binding domains: E, D, A, B and C [12]. The high resolution structures of the B domain [13] and the B domain bound to IgG [14] have been solved. The B domain binds the Fc region of IgG, leaving the antibodies free to bind antigen [15]. Two mutations (A1V and G29A) have being introduced into the B domain to create what is termed the Z domain [16], A1V creates a convenient DNA cloning site and G29A removes a hydroxylamine-sensitive site [16].

For surface assembly we use the β-barrel transmembrane domain (residues 1 to 171) of outer membrane protein A (tOmpA) [17,18]. In ctOmpA this is circularly permuted in extracellular loop 1, has 6xHis tag at the N-terminus and a cysteine on the 'periplasmic' side to

* Corresponding author. Fax: +44 191 222 7424.
E-mail address: j.h.lakey@ncl.ac.uk (J.H. Lakey).
[1] Present address: Bragg Institute, Australian Nuclear Science and Technology Organisation, Locked Bag 2001, Kirrawee DC, NSW 2232, Australia.

0142-9612/$ – see front matter © 2011 Elsevier Ltd. All rights reserved.
doi:10.1016/j.biomaterials.2011.01.026

allow binding to gold [8,10]. This acts as a scaffold to which we can fuse motifs for different biosensor applications [10] such as the two Z domains which were fused to the N-terminus of ctOmpA creating the protein ZZctOmpA. The assembly of the sensing layer consists of a protein immobilisation step followed by the addition of a thiol-containing amphiphile which completes the self-assembled monolayer [8]. This amphiphile has been shown to stabilise the bound protein [8,9] and in this work has a poly(ethylglycol) head group which reduces non-specific binding to the remaining surface [19].

The self-assembly of biosensors in this way is simple but there are few methods to assess the quality of the layer in terms of surface coverage and thickness. In previous studies we have shown that neutron reflection can be used to probe this class of thin organic/protein layers [20–22]. In particular we showed that the increase in thickness upon antibody binding to ZZctOmpA could be easily detected [21]. Here we combine surface plasmon resonance (SPR) and neutron reflection to probe more deeply the assembly of the protein array, antigen binding capacity and the structural orientation of the bound antibody/antigen layer. The result is a clear, layer by layer, model which provides an unusually clear picture of an engineered biosensor surface.

2. Materials and methods

2.1. Materials

General reagents were either from Melford Laboratories (Ipswich, Suffolk, UK) or from Sigma–Aldrich (Poole, Dorset, UK) unless other wise stated. Antibodies and human serum albumin were from Sigma–Aldrich. Chromatography columns were from GE Healthcare (Chalfont Saint Giles, Buckinghamshire, UK). ThioPEG was purchased from Prochimia Surfaces (Sopot, Poland).

2.2. Molecular biology

The pORLA9 plasmid contains the gene encoding for the circularly permuted ctOmpA [23] such that the N and C termini occur in external loop 1. The Z domain genes were amplified by PCR from plasmid pEZZ [24] and cloned into pORLA9 between the histidine affinity tag and the N-terminus of ctOmpA thus creating (His_6-)ZctOmpA and (His_6-)ZZctOmpA.

2.3. Protein expression and purification

The ctOmpA, ZctOmpA and ZZctOmpA proteins were expressed as inclusion bodies in *E. coli* BL21(DE3) cells grown in LB media induced by the addition of IPTG at 1 mM when the cells were at OD_{600} of 0.6–0.7 in flask cultures shaken at 180 rpm and 37 °C. After 3 h induction the cells were harvested by centrifugation at 6000×*g* for 10 min. The cells were disrupted by incubation overnight at −20 °C in a detergent solution of Bugbuster (Novagen, Nottingham, UK) (using 10 mL for every gram of wet cell pellet) which was supplemented with DNase, RNase and lysozyme. The inclusion bodies were isolated by centrifugation at 12 000×*g* for 20 min and washed three times by homogenisation in a 1 in 10 dilution of Bugbuster in deionised water followed by centrifugation at 12 000×*g* for 20 min. The proteins were then purified from inclusion bodies as previously described [25]. Pure protein fractions were concentrated to a volume of 1 mL using a Vivaspin 10 000 molecular weight cut-off spin concentrator. The proteins were refolded by slowly diluting the protein plus urea 1:10 into refold buffer (20 mM Tris–HCl pH 8.0, 1% (w/v) OG, 0.1 mM EDTA and 1 mM DTT) and left to incubate for 48 h at 37 °C to allow for complete refolding. Residual urea was removed by buffer exchange using a PD10 column equilibrated with refold buffer with 1 mM TCEP replacing DTT.

2.4. Circular dichroism

Circular Dichroism spectroscopy was carried out using 0.02 cm pathlength demountable cuvettes in a Jasco J-810 spectropolarimeter. The protein concentration was determined by protein absorbance at 280 nm and circular dichroism was scanned from 250 nm to 185 nm ten times, averaged and a buffer blank was subtracted. The circular dichroism was expressed as $\Delta\epsilon$ and imported into the CDSSTR website for secondary structure content analysis [26].

2.5. Preparations of proteins and filling molecules for surface deposition

Before deposition on gold, TCEP reducing agent was added to the protein and the filling molecules at a final concentration of 1 mM and incubated at room temperature for >10 min. The filling molecule, 1-mercaptoundec-11-yltriethylene glycol (thioPEG), diluted in a solution of 1% (w/v) OG, 20 mM Tris–HCl pH 8.0 and 1 mM TCEP was heated to 50 °C before deposition to ensure complete dissolution.

2.6. Surface plasmon resonance

Surface Plasmon resonance (SPR) experiments used Biacore X and 2000 instruments and Au sensor chips. The gold surface of the chip was cleaned by incubation for 15 min in an acid piranha solution (70% (v/v) concentrated sulphuric acid 30% (v/v) hydrogen peroxide) by incubation for 15 min. The surface was then cleaned with 1% (v/v) Hellmanex (Hellma UK, Southend on Sea, Essex, UK) and rinsed with deionised water. The chip surface was passivated by 1% (v/v) BME solution in ethanol for 10 min followed by washing with 1% (w/v) SDS and distilled water [8,27]. The running buffer was phosphate buffered saline (PBS, 20 mM sodium phosphate pH 7.6, 137 mM NaCl and 2.7 mM KCl). The protein was injected in a typical volume of 50 μL at a flow rate of 5 μL min^{-1} followed by injections of 1% (w/v) SDS to remove non-specifically bound protein before the filling molecule, thioPEG, was deposited. Three times 50 μL of 0.25 mg mL^{-1} thioPEG in a solution of 1% OG at a rate of 5 μL min^{-1} was used for each deposition, with a wash of 1% (w/v) SDS between each deposition to remove non-specifically bound thioPEG. Antibodies (IgG) and antigen (human serum albumin, HSA) were diluted in PBS and injected into the flow cell at a rate of 2 μL min^{-1}. The regeneration buffer was 100 mM glycine pH 2.0.

The BIAcore 2000 generated kinetic data to measure the equilibrium dissociation constants for ZZctOmpA arrays and immunoglobulins, 20 μL of IgG at various concentrations were flowed over a ZZctOmpA array at 10 μL min^{-1}. Flow rates of 5, 10 and 20 μL min^{-1} did not alter the association rate (Supplementary Fig. S1). IgG dissociation rate from the array, in a flow rate of 10 μL min^{-1} buffer, was measured for 20 min before regeneration. All data was corrected by subtracting appropriate blanks. After IgG injection is completed the decrease in response can be considered purely a dissociation event and the dissociation rate constant is calculated using Eq. (1) [28]:

$$Ln(R_0/R_n) = k_{off}(t_n - t_0) \quad (1)$$

Where R_0 is the response at time zero, t_0, R_n is the response at time t_n and k_{off} is the dissociation rate constant. The gradient of a plot of $Ln(R_0/R_n)$ versus $(t_n - t_0)$ is the dissociation rate constant. During the IgG injection phase the change in response is a function of both the IgG association and dissociation from the ZZctOmpA array and equation (2) is used to calculate the association rate constant, k_{on}:

$$dR/dt = (k_{on}CR_{max}) - \left\{\left[(k_{on}C) + k_{off}\right]R\right\} \quad (2)$$

Where dR/dt is the relative change in response per second, R is the response at any given time, C is the concentration of IgG and R_{max} is the maximum response. The gradient for a plot of dR/dt versus R for each concentration measured is calculated and then the gradient of a second plot of slope versus IgG concentration is the association rate constant. The equilibrium dissociation constant, K_d is thus:

$$K_d = k_{off}/k_{on} \quad (3)$$

Experiments were measured in triplicate and the standard error of the mean (SEM) is quoted as the error values.

2.7. Neutron reflection

Polarised reflection experiments were carried out on the CRISP reflectometer at ISIS, Rutherford Appleton Laboratory, UK or on the NG-1 reflectometer at the NIST Centre for Neutron Research, Maryland, USA. Both reflectometers were used in polarised mode. The surfaces were made at NIST (NG-1) or by Microsystems and Nanotechnologies, Lisbon, Portugal (CRISP). The silicon substrate was coated with an 80 to 140 Å layer of μ-metal (an alloy of 75% iron, 15% nickel with traces of copper and molybdenum) and then with a 150 to 200 Å layer of gold by either magnetron sputtering (NG-1) or ion beam deposition (CRISP). The substrates were 50/100 mm in diameter and 5/10 mm thick for NG-1/CRISP. Once removed from vacuum the surfaces were washed with >18 MΩ water, followed in order by ethanol (AnalaR grade), 1% (v/v) BME in ethanol, 1% (w/v) SDS, water and ethanol again and dried under a stream of nitrogen gas. The protein array was assembled by placing gold surface in a glass Petri-dish with lid and pouring the protein solution on to cover the whole gold surface (7–9 mL at a concentration of 0.25 mg mL^{-1}). After 1 h at room temperature the protein solution was removed and the surface washed with 1% (w/v) SDS and then >18 MΩ water. The original protein solution was returned to the surface and this cycle was repeated three times to gain maximum surface coverage. Then thioPEG was added to cover the surface and the lid replaced. After 1 h the surface was once again washed with 1% SDS and water and this cycle was also repeated three times. The surface was then mounted into its cell and placed on the beamline where all subsequent additions of antibody, antigen, change of buffer etc were carried out *via* the cell's inlet and outlet values using a syringe and ×10 excess of the cell's void volume.

In reflectivity experiments the intensity of the reflected neutrons with respect to the intensity of the incident neutrons (reflectivity) is measured as a function of momentum transfer, Q which is defined as

$$Q = 4\pi \sin\theta/\lambda \quad (4)$$

where θ is the angle of incidence and λ is the neutron wavelength (for a review see [29]). In these experiments the technique of magnetic contrast neutron reflection was used as previously described [22,30]. This increases the resolution such that even the BME layer on gold can be clearly resolved [22]. Briefly the sample is placed in an external magnetic field to align the magnetic domains in the μ-metal layer. Spin up or spin down polarised neutrons then reflect differently from the magnetic layer between the gold surface and the silicon substrate. This means that each biological sample provides two separate contrast sets and therefore two independent data sets for the one biological layer which can yield a unique solution for modelling of the scattering length density (SLD) profile. As CRISP is a time-of-flight instrument viewing a hydrogen moderator at the ISIS pulsed neutron source with a white beam of neutrons ($\lambda = 1.5$–6.5 Å), the sample in a horizontal geometry, was measured at three angles (0.35°, 0.8° and 1.8°) using D_2O and four angles (0.2°, 0.35°, 0.8° and 1.8°) when using other subphases. The beam defining slits were adjusted between incident angles so that a constant sample area was illuminated. NG-1 is on a 20 MW reactor source facing a moderated cold neutron guide and has a fixed wavelength of 4.75 Å. The sample was in a vertical geometry and to achieve the full Q range an angle of incidence of 0.23°–7.2° was used.

The raw data from both instruments was reduced so that the collected reflectivity profiles were on an absolute scale and could be analysed using the same software packages. The fitting of the data was carried out using GA_refl [31,32]. Multiple data sets with different magnetic and isotopic contrasts are fitted simultaneously with best fits analysed using a Monte Carlo (MC) resampling procedure [22,33,34].

3. Results

3.1. Protein morphology

OmpA is an eight stranded β-sheet protein [35], whilst ZZctOmpA is circularly permutated and contains two helix-rich Z domains [36]. The secondary structure contents of these known protein structures were calculated using STRIDE [37]. By CD, ctOmpA has a characteristic β-sheet signal whilst ZZctOmpA has a stronger negative signal consistent with its α-helix content (Fig. 1); ZctOmpA has a intermediate CD spectrum (Fig. 1). The CD spectra were analysed for secondary structure content by the CDSSTR algorithm [26] (STRIDE result in brackets); ctOmpA = 9% (0%) helix and 44% (53.4%) strand and ZZctOmpA = 26% (27.4%) helix and 29% (32.2%) strand. Thus the engineered protein has the expected solution structure.

3.2. Surface assembly

The SPR trace (Fig. 2) shows the assembly of a ZZctOmpA layer using the BIAcore X instrument from a 0.2 mg mL^{-1} protein solution. After three depositions/washes the thioPEG filling molecule is added at a concentration of 0.25 mg mL^{-1} in detergent micelles (1% (w/v) OG). Between each thioPEG application the surface was washed with 1% (w/v) SDS to remove non-specifically bound material. The specifically bound protein gave responses between 1000 and 1800 resonance units (RU). This corresponds to a surface coverage of 1.74–3.14 × 10^{10} protein molecules mm^{-2} (assuming 1 RU = 1 pg mm^{-2} [38]).

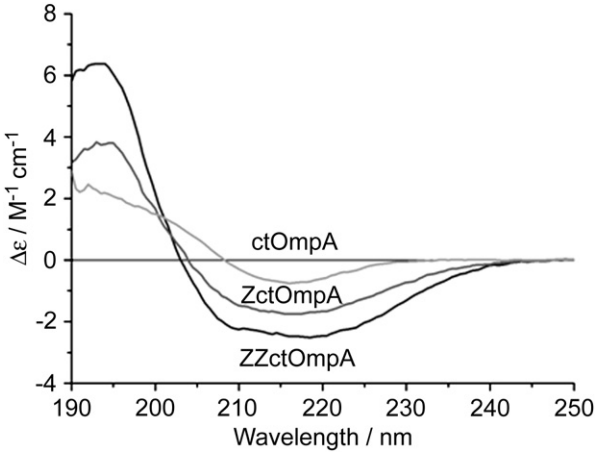

Fig. 1. Circular dichroism of the ctOmpA proteins. ZZctOmpA (black line), ZctOmpA (red line) and ctOmpA (green line). The circular dichrosim becomes more negative at 220 nm as more α-helix is present. Scans were collected from 250 nm to 190 nm in a 0.02 cm cuvette at protein concentrations of 0.244 mg mL^{-1} (ZZctOmpA), 0.254 mg mL^{-1} (ZctOmpA) and 0.321 mg mL^{-1} (ctOmpA).

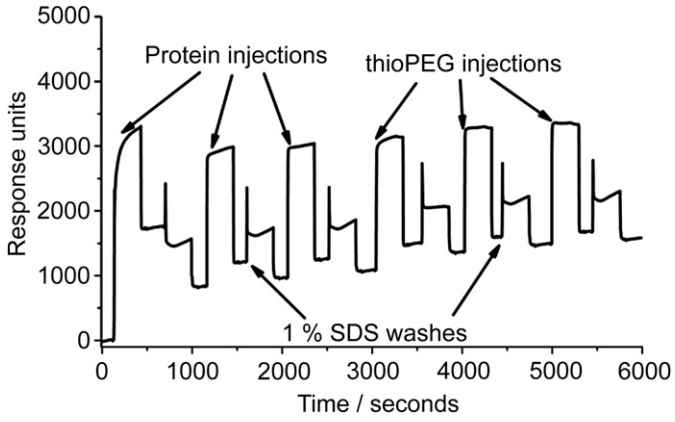

Fig. 2. Assembly of ZZctOmpA onto a gold surface. The assembly was carried out on a BIAcoreX using an Au sensor chip. 25 μL of ZZctOmpA (0.205 mg mL^{-1}) was injected at 5 μL min^{-1} into the flow cell. Protein bound non-specifically was removed with a wash of 1% (w/v) SDS (25 μL at 5 μL min^{-1}). The protein deposition was repeated three times. The space between the immobilised ZZctOmpA molecules was filled by a deposition of a lipid mimic, thioPEG at 0.25 mg mL^{-1} in 1% (w/v) OG, 20 mM Tris–HCl pH 8.0 and 1 mM TCEP at 40 °C. 25 μL was injected at a flow rate of 5 μL min^{-1}. As with the protein deposition, non-specifically bound thioPEG was removed with a wash of 1% SDS. The thioPEG deposition was repeated three times.

The surface assembly monitored using neutron reflection [21] showed that an average surface coverage[2] of 15–20% is achieved (Fig. 3) however a surface coverage of up to 40% is possible [21]. The coverage of the thioPEG was found to vary between 63% and 72% depending on the prior protein surface coverage. Whilst SPR shows how much thioPEG is deposited, the use of neutron reflection shows how crucial the filling molecule is to the integrity of the protein array. The fitting of the neutron reflection data from a gold surface with just BME and protein deposited shows that the orientation of the ZZctOmpA is ill-defined. Overall the protein is shorter and there is a high surface roughness (Fig. 3). After the thioPEG is deposited onto the surface ctOmpA-ZZ adopts a uniform orientation (Fig. 3).

The total height of the ZZctOmpA plus thioPEG array is 120 Å but it is possible to deduce the structure of ZZctOmpA molecule within the array by using different experiments. An array of ctOmpA was measured using MCNR (Fig. 4a) and the height of ctOmpA was found to be 60 Å (Fig. 4b), which is in agreement with the published crystal structure of tOmpA (57 Å) [17]. A deposition of only thioPEG was carried out on the surface and this showed that the thioPEG can achieve a surface coverage of 88% and 22 Å thickness when no protein is deposited. These measurements were used to define where the protein components are in the derived SLD profile.

3.3. The antibody layer

The antibody layer was analysed in four sequential stages, the addition of polyclonal rabbit anti-HSA IgG which binds to the ZZctOmpA molecule, a wash to remove free antibody, injection of

[2] Surface coverage is calculated by comparing the fitted SLD value from the ZZctOmpA only layer with the theoretical SLD for a 100% ZZctOmpA layer.

Table 1
The results of the fitting for the antibody layer. The numbers in brackets are the errors calculated using MC analysis. The overall roughness of the layer was 30 Å.

Addition to ZZctOmpA array	Thickness/Å	SLD/$\times 10^{-6}$ Å^{-2}
Polyclonal anti-HSA IgG	126 (1.0)	5.47 (0.02)
IgG plus HSA	163 (1.0)	5.69 (0.03)
IgG and HSA plus anti-rabbit IgG from goat	210 (6.7)	5.60 (0.03)

antigen (HSA) and a regeneration step to remove antibody and antigen (Fig. 5a). SPR showed a very large response when antibody is injected. Non-specific binding was investigated using ctOmpA as a control and Fig. 5b shows the comparison of binding between ctOmpA and ZZctOmpA for two extreme concentrations of rabbit polyclonal anti-HSA IgG. At the very high IgG concentration of 108 μg mL^{-1} the amount of non-specific binding to ctOmpA is 20% of the ZZctOmpA result. At the low IgG concentration of 270 ng mL^{-1} binding to ZZctOmpA is not significantly greater than to ctOmpA. As expected no binding was observed to a surface just consisting of the thioPEG filling molecule (data not shown) [19].

Using a direct fitting approach for BIAcore data similar to that used by Jendeberg et al. [28] (see Section 2) the equilibrium dissociation constants for two different IgG subclasses binding to the ZZctOmpA were deduced (Table 2) [28,39]. The IgG samples were, rabbit polyclonal anti-HSA IgG and mouse monoclonal anti-HSA IgG2a. The association rate constants for ZZctOmpA binding of the two IgG subclasses and the SPR binding curves look similar (Fig. 6). The dissociation rate constants, however, are an order of magnitude different (Table 2) and in Fig. 6 the mouse monoclonal IgG2a has a much steeper descent than that of the rabbit polyclonal IgG. The small dissociation constant of the ZZctOmpA: rabbit IgG means that the half-life of the complex is over 24 h. This makes the antibody-binding array suitable for neutron reflection data collection (<10 h).

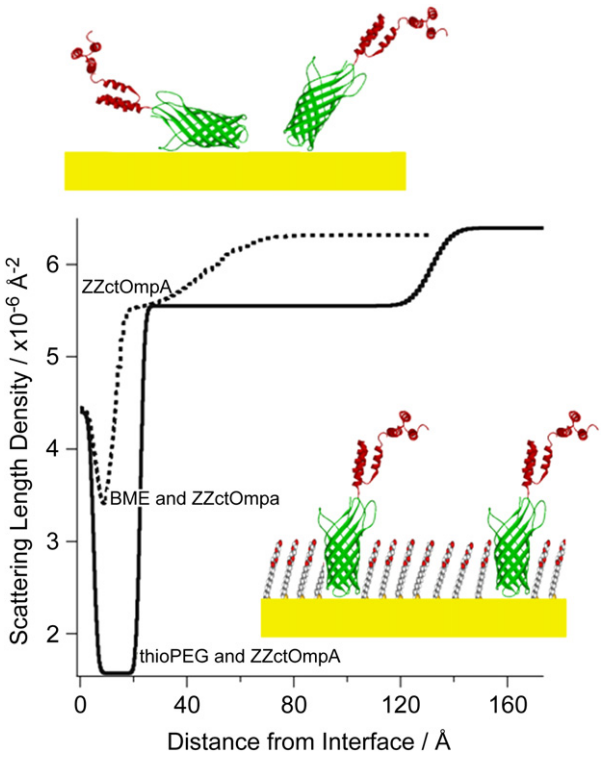

Fig. 3. The SLD profiles of ZZctOmpA immobilised to gold surface before (dotted line) and after (solid line) thioPEG deposition. The figure shows that when there is only protein and BME present on the surface the protein only layer is ill-defined. Once the filling molecule, thioPEG is added the protein is able to adopt a uniform orientation and the expected thickness of ZZctOmpA is observed.

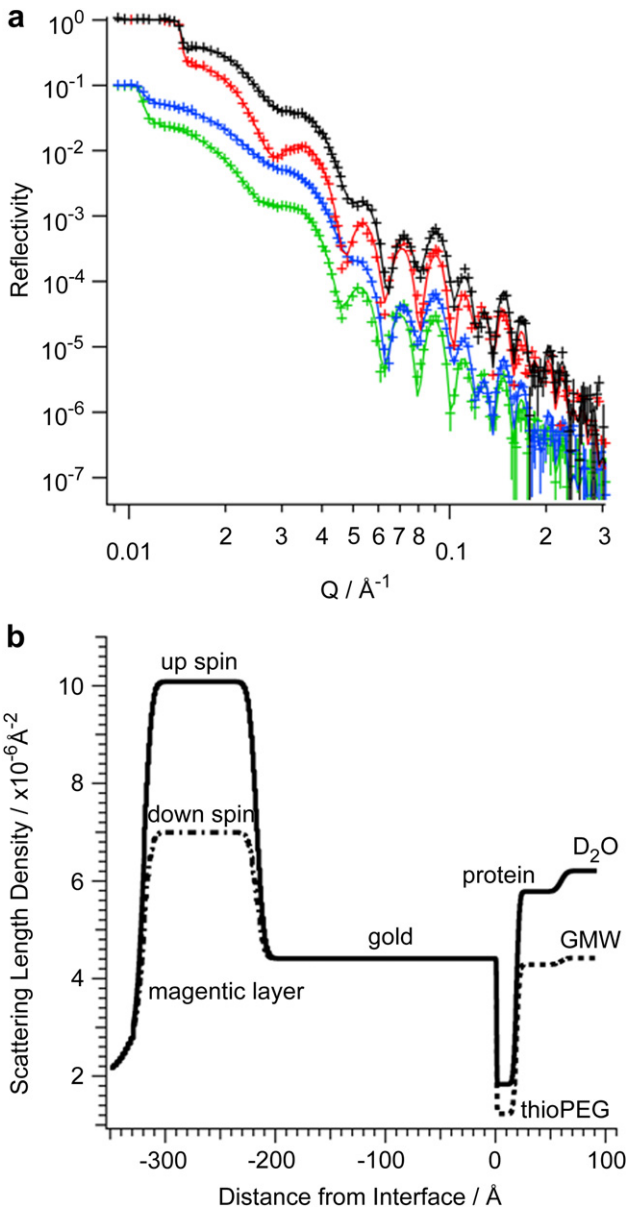

Fig. 4. a) The reflectivity of an array of ctOmpA in a D_2O (black spin up and red spin down) and gold matched water (GMW) where the SLD is matched to gold (blue spin up and green spin down). The crosses with error bars are the collected data and the solid lines the fits. The GMW data is offset for clarity. b) The corresponding SLD profile of the ctOmpA array with the gold–membrane interface set at 0 Å. The SLD of the μ-metal from spin down neutrons and the membrane layer in GMW are shown as dashed lines.

For neutron reflectivity experiments the rabbit polyclonal anti-HSA IgG was added to the cell at 30 μg mL^{-1}, a concentration at which binding to the ZZctOmpA array is highly specific (Fig. 5b). The cell was then flushed with buffered D_2O to remove excess antibody before data collection. A comparison of the reflectivity profiles before and after IgG addition showed a difference after the critical edge and in the shape of the first fringe (Supplementary Fig. S6). These are characteristic of immobilising hydrogenous material onto gold surfaces [21,22]. There are additional and similar changes observed when antigen and then a secondary antibody are added (Supplementary Fig. S7). After the addition of the antibody

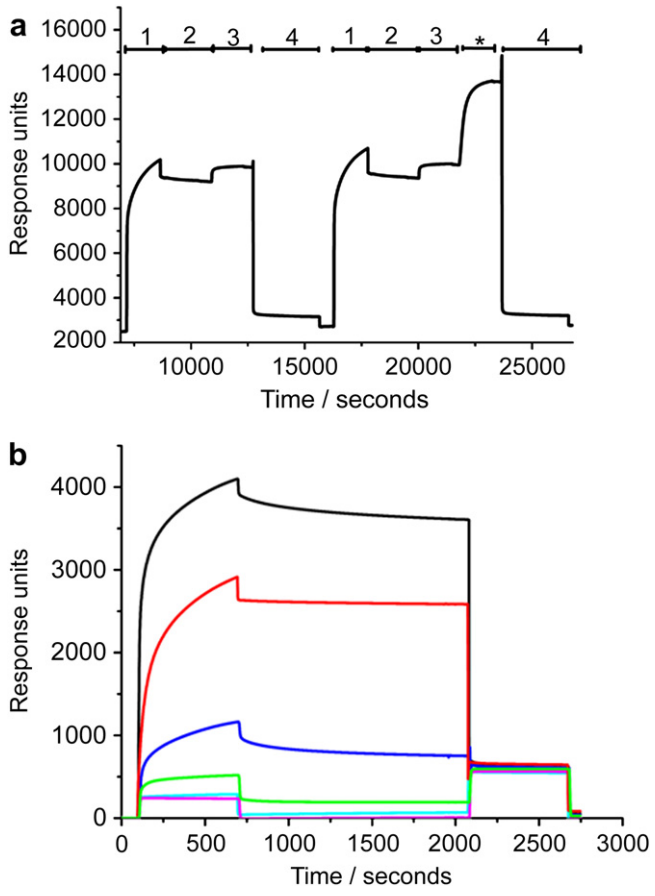

Fig. 5. a) Assembly of antibody and antigen on a ZZctOmpA array. Rabbit polyclonal anti-HSA IgG at a final concentration of 370 nM in PBS was injected into the flow cell at 2 μL min^{-1} (section 1). The array was then washed with PBS running buffer to remove any non-specifically bound IgG (section 2). The antigen was human serum albumin at a concentration of 0.1 mg mL^{-1} in PBS which, was injected after the antibody wash (section 3). The protein surface can be regenerated with a wash of 100 mM glycine pH 2.0 into the flow cell (section 4). The antibody and antigen assembly can be repeated after the regeneration step. On the second antibody addition in this figure a secondary antibody was bound (section *) which was anti-rabbit IgG produced in goat at a concentration of 220 nM in PBS. b) The non-specific binding of rabbit polyclonal anti-HSA IgG. The binding of the antibody was compared between ZZctOmpA (black, red and cyan) and ctOmpA (blue, green and magenta) at three different concentrations: 108 μg mL^{-1} (black and blue), 27 μg mL^{-1} (red and green) and 270 ng mL^{-1} (magenta and cyan). The surface was washed with PBS and regenerated with 100 mM glycine pH 2.0.

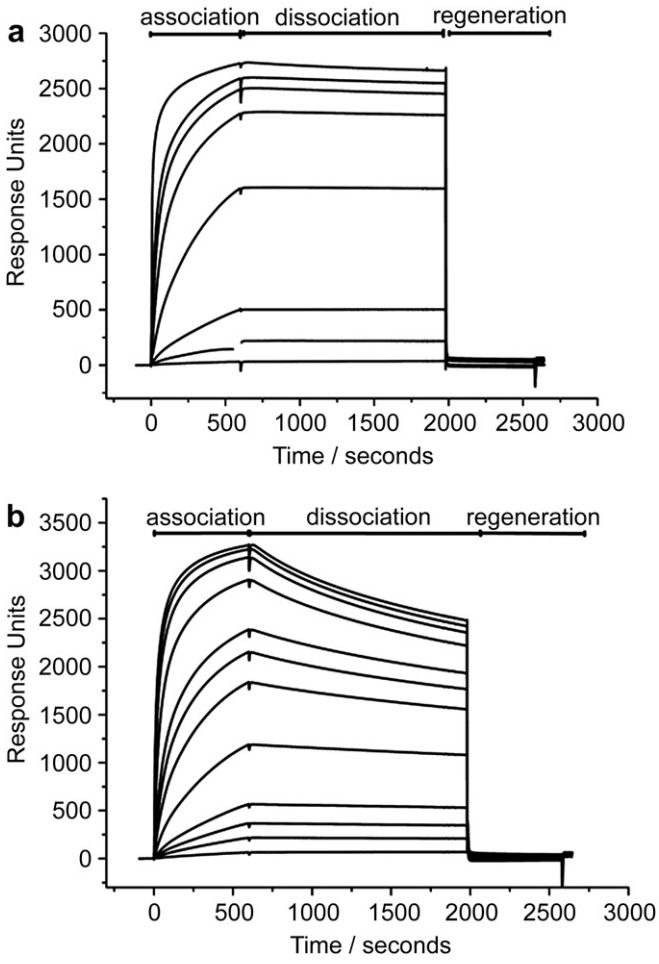

Fig. 6. Binding of rabbit polyclonal anti-HSA IgG and mouse monoclonal anti-HSA IgG2a to a ZZctOmpA array. A ZZctOmpA array in Fc1 and ctOmpA array in Fc2 were assembled *in situ* on an Au chip in a BIAcore2000. Different concentrations of anti-HSA IgG were immobilised to the surface at 10 μL min^{-1} with a contact time of 10 min. The dissociation time was 20 min. Before the next antibody concentration was injected the surface was regenerated each time with 100 μL of 100 mM glycine pH 2.0. Non-specific binding to ctOmpA and the buffer background was subtracted from the data. a) Rabbit polyclonal anti-HSA IgG. The concentrations of antibody used were 5.4 nM, 7.2 nM, 18 nM, 36 nM, 54 nM, 72 nM, 359 nM and 717 nM b) Mouse monoclonal anti-HSA IgG2a. The concentrations of antibody used were 1.2 nM, 2.4 nM, 3.6 nM, 4.8 nM, 12 nM, 24 nM, 36 nM, 48 nM, 121 nM, 242 nM, 363 nM and 484 nM.

a three layer model of the biological component is needed to fit the scattering length density profiles (Fig. 7). These consist of the thioPEG plus ZZctOmpA layer, a ZZctOmpA only layer and the ZZctOmpA plus antibody layer; all three contain solvent. The combined thickness of the thioPEG plus ZZctOmpA layer and the ZZctOmpA only layers is 60 Å and equals the scaffold protein part (ctOmpA) of the ZZctOmpA molecule. The antibody and ZZctOmpA layer is the thickest at 126 Å. The dimensions of the IgG antibody are 143 × 77 × 40 Å^3 [40] and the distance from the antibody-binding site to the Z domain binding region is 110 Å (all distances as measured on Swiss PDB viewer [41]). A distance of 128 Å then suggests an orientation where the antibody is upright with the antibody-binding site facing away from the surface. This improves on previous data where only the total bio-layer (ZZctOmpA plus IgG) thickness was defined to be 187 Å but the IgG thickness was not defined [21]. From the fitted profiles, the scattering length density difference between the ZZctOmpA only layer and the antibody layer is not large, 5.82 × 10^{-6} Å^{-2} and 5.47 × 10^{-6} Å^{-2} respectively (Fig. 7 and Table 1). The theoretical SLD between them is not large either (SLD for ZZctOmpA and IgG in D_2O are 3.076 × 10^{-6} Å^{-2} and 3.371 × 10^{-6} Å^{-2} respectively), and therefore SLD changes will result largely from solvent (D_2O) replacement by protein. Nevertheless for the best fits it was necessary to model the ZZctOmpA and antibody SLD as two distinct layers. For the same

Table 2
The association and dissociation rate constants and the dissociation equilibrium constant of rabbit polyclonal and mouse monoclonal anti-HSA IgG to ZZctOmpA arrays. The results show the standard error in the mean (SEM) from three independent experiments.

Antibody	k_{on}/M^{-1} s^{-1} (±SEM)	k_{off}/s^{-1} (±SEM)	K_d/nM (±SEM)
Rabbit polyclonal anti-HSA IgG	2.03 × 10^5 (±4670)	2.74 × 10^{-5} (±8.11 × 10^{-8})	0.137 (±0.017)
Mouse monoclonal anti-HSA IgG2a	3.74 × 10^5 (±7312)	2.91 × 10^{-4} (±1.78 × 10^{-6})	0.778 (±0.243)

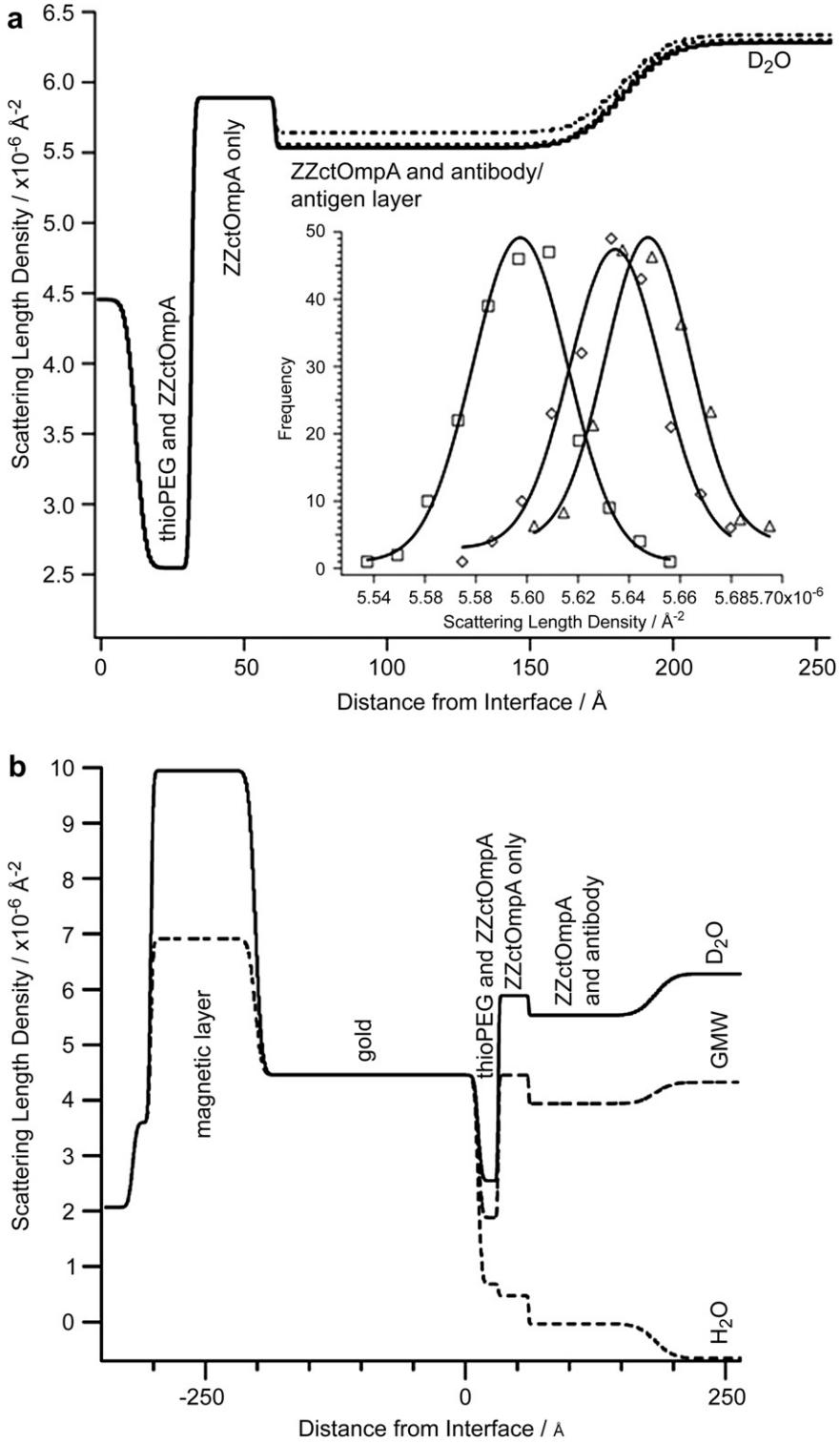

Fig. 7. a) The SLD profile of a ZZctOmpA array (from the reflectivity profiles in Supplementary Fig. S6) with the addition of rabbit polyclonal anti-HSA IgG (solid line), followed by the addition of antigen, HSA (dotted line). The final addition to the array is a secondary antibody, anti-rabbit IgG produced in goat (dashed line). All profiles are of the D_2O only subphase. The inset show the output from the MC analysis for the SLD of the ZZctOmpA antibody layer with rabbit anti-HSA IgG only (squares), after the addition of HSA (diamonds) and the final addition of anti-rabbit IgG produced in goat (triangles). The Gaussians are drawn as a guide. b) The SLD profile of rabbit anti-HSA IgG bound to an array of ZZctOmpA under magnetic and solvent contrasts.

reason there is also very little density contrast between the IgG antibody and the HSA antigen due to their very similar SLD values. The SLD is the sum of the product of the volume fraction and SLD for each component in the layer i.e. for the antibody layer this will be IgG and solvent. Assuming that the antibody layer is homogenous, the surface coverage of the IgG is 35%. Considering that a typical volume fraction in a protein crystal is typically 50–60% this is dense packing and further suggests that the only conformation that the antibody could adopt is an upright orientation on the surface (Fig. 8).

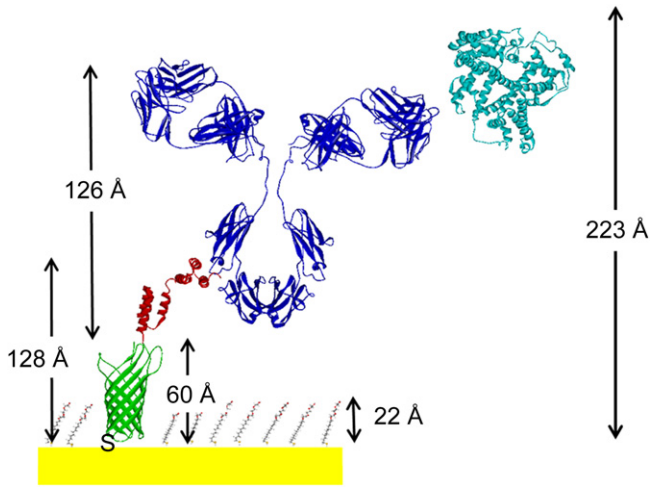

Fig. 8. A schematic of the proposed orientation of antigen bound IgG bound to gold immobilised ZZctOmpA. The ZZctOmpA molecule is immobilised to gold *via* a thiol-gold bond between the gold surface and a cysteine residue (denoted by a letter 'S') in turn four of the tOmpA domain (green β-barrel section). The tOmpA is insulated by a 22 Å layer of thioPEG. The one of the Z domains (red) of ZZctOmpA will bind IgG at its constant region leaving the variable region to bind antigen which in this case was HSA (light blue).

3.4. Antigen binding

The HSA antigen binding detected by SPR (Fig. 5a, section 3) is lower than expected especially if the IgG is in an upright position exposing both antigen binding sites to the solution. The response to 0.1 mg mL^{-1} HSA injection is much weaker to that when IgG is added. The probable reason for this is that we used a complete IgG fraction of a polyclonal antibody in which not every IgG molecule will have anti-HSA specificity. When binding HSA to bound mouse monoclonal anti-HSA IgG2a no improvement in the amount of HSA bound was observed (Supplementary Fig. S4) and this is likely due to the poor affinity for IgG. Additionally, the molecular mass of HSA is 66 000 g mol^{-1} compared to an IgG molecular mass of 150,000 g mol^{-1} and thus if HSA saturated all of the IgG molecules the response of the HSA injection would be less than half of the IgG response. The SPR signal falls with distance from the surface and maybe significantly less sensitive if the antigen binds 200 Å from the gold–water interface. Fig. 5a and Supplementary Fig. S4 clearly show that although the HSA has saturated the available antigen binding sites (Fig. 2) the amount of HSA binding to IgG is lower than expected. In Fig. 3 there are 8.47×10^9 HSA molecules per mm^2 bound compared to 1.53×10^{10} anti-HSA IgG molecules bound per mm^2. When assembling the biological layers for neutron reflection studies we cannot monitor the assembly in real-time, so a high concentration of HSA was used (0.3 mg mL^{-1} as opposed to the 0.1 mg mL^{-1} used for the SPR experiments) to saturate antibody. The HSA solution in deuterated PBS buffer was incubated in the cell for 30 min and then washed with deuterated PBS buffer before data collection. From the neutron reflectivity data there appears to be little change in the profiles between that of the rabbit polyclonal anti-HSA IgG bound only and that with the HSA also bound (Supplementary Fig. S7). However the modelling does show difference in the antibody layer (Fig. 7a). For the best fitting results the IgG with bound HSA had to be treated as a single layer. Separation of the IgG and the HSA into two distinct layers resulted in a poorer fit (χ^2 of 11.9 and 5.98 when the antibody and HSA are treated as two and one layer respectively). Table 1 shows that upon HSA addition the antibody layer increases by 40 Å but the layer thickness is ill-defined due to the surface roughness of the layer (30 Å) (Table 1 and Fig. 7a). The SLD of the antibody layer also increases upon HSA binding which corresponds to a decrease in the protein volume fraction.

3.5. Secondary antibody

The last addition to complete the array was a secondary antibody, anti-rabbit IgG produced in goat. The SPR trace (Fig. 5a, section *) shows a strong response upon injection of 30 μg mL^{-1} anti-rabbit IgG produced in goat in PBS. The trace shows that 1:1 binding of primary to secondary antibody is achieved. It has been shown previously that IgG produced in goat binds very poorly to Z domains (Antibody Purification Handbook, page 48, GE Healthcare) and only 122 RU of anti-rabbit IgG binding to ZZctOmpA was observed when no rabbit polyclonal anti-HSA IgG was present.

Addition of the anti-rabbit IgG did not show much change in the reflectivity upon its binding to the array (Supplementary Fig. S7). However an observable change is seen in the scattering length density after the modelling has been completed (Fig. 7a). The volume fraction of the antibody layer is high at 0.25 which may mean that the antibody layer is very compacted and the anti-rabbit IgG cannot penetrate to reach its binding site.

4. Discussion

The engineered ZZctOmpA protein has the expected secondary structure content in detergent solution (Fig. 1). When it initially binds to a gold surface it can form many orientations on the gold as revealed by the high degree of roughness in the fitted SLD plots. The ctOmpA scaffold has one cysteine group in turn four of its structure which means that it is anchored to the gold surface by only one thiol-gold bond. This is unlike trimeric OmpF which has three thiol groups and thus forms a much more rigid structure before the filling molecule is added [9,22]. Once the array is completed with the filling molecules the proteins adopt a defined perpendicular orientation (Fig. 3). This is shown in the expected thickness of the immobilised protein, decreased roughness and the correct function of an IgG binding array.

Analysis of the SPR data shows that ZZctOmpA arrays can bind immunoglobulins with sub nanomolar affinities and there is a difference between rabbit and mouse IgG affinity. The binding affinities are consistent with biosensor data from Z domain immobilised to a dextran-coated gold surface [28]. The density of ZZctOmpA makes rebinding events likely and, due to likely mass transport effects at this density of protein, global fitting of the binding data is inapplicable. Thus we do not present data for the affinity of the proteins but rather the apparent affinity of the array. In this case direct fitting is the most appropriate method to determine whether the dissociation rate is sufficiently low to allow long data collections on a neutron reflectometer. The slow dissociation rates confirmed that the arrays are suitable for both diagnostic tests using antibodies and for neutron studies over several hours. The neutron reflection data using magnetic contrast provides accurate and reproducible measurements of the antibody layer thickness. The rabbit polyclonal anti-HSA IgG bound to ZZctOmpA is at least 126 Å thick, which although less than the longitudinal length of IgG in solution can only suggest an IgG orientation where the variable domains are pointing away from the surface and in the optimal position to bind HSA (Fig. 8). We know from the X-ray crystallography structure that the Z domain binds to IgG at its constant region [14] and therefore in this system the antigen-binding regions face away from the surface. The surface roughness of the antibody layer is 30 Å and this may describe the flexibility of the Z domains. The volume fraction of the rabbit polyclonal anti-HSA IgG at 0.28 (with the remaining volume being water) suggests a densely packed IgG layer comparable with systems where IgG has been adsorbed to

silica or polymer surfaces [42–44]. In this case the density of the antibody layer showed many antibody orientations as shown by Xu et al. [44,45] and the different orientations were deduced by splitting the antibody layer into three separate layers each with a varying volume fraction of IgG. In the system described in this paper there are already six layers before the antibody is added. Adding an additional three antibody layers would lead to a dramatic decrease in the ratio of fitted parameters to data points. It then becomes difficult to interpret the derived SLD profiles. Here use of different solvent contrasts in combination with magnetic contrast [22] results in the best χ^2 values (Figs. 4 and 7b and Supplementary Fig. S5). Adding extra constraints to the model through the use of more contrasts helps remove ambiguities about the orientation of the antibody layer. The improved fitting is achieved by assuming the thickness of the layer remains constant as the contrast changes and allowing the SLD of the antibody layer to vary with each contrast.

It has been shown by equilibrium dialysis [46] and isothermal titration calorimetry [47] that when IgG is free in solution the stoichiometry of IgG to antigen is 1:2. However in this work the ratio of antibody to antigen is 1:0.534 even though the HSA injection reaches a plateau and is saturating (Fig. 5a). It has been seen before when IgG antibodies are immobilised to a surface that their antigen binding capacity has been reduced and in some cases this reduction is more than 50% [48–50]. The possibility of non-HSA specific antibodies in the IgG sample cannot be eliminated.

5. Conclusion

The experiments show that a gold immobilised, antibody-binding, membrane protein retain its function and binds rabbit polyclonal anti-HSA IgG in an upright orientation facing away from the surface. This achieves the highest possible density of IgG and provides a basis for very sensitive immunodiagnostic devices where the antigen needs to be bound at high density close to the transducer surface.

Acknowledgements

The authors would like to thank the Biotechnology and Biological Sciences Research Council, the Science and Technology Facilities Council and Orla Protein Technologies Ltd for funding. We thank ISIS Neutron Facility and NIST Centre for Neutron Research for the award of beam time. The identification of any commercial product or trade name does not imply recommendation or endorsement by the National Institute for Standards and Technology.

Appendix. Supplementary data

Supplementary data related to this article can be found online at doi:10.1016/j.biomaterials.2011.01.026.

References

[1] Cornell BA, Braach-Maksvytis VLB, King LG, Osman PDJ, Raguse B, Wieczorek L, et al. A biosensor that uses ion-channel switches. Nature 1997;387:580–3.
[2] Hong J, Yoon DS, Park M, Choi J, Kim TS, Im S, et al. A dielectric biosensor using the capacitance change with AC frequency integrated on glass substrates. Jap J Appl Phys 2004;43:5639–45.
[3] Leatherbarrow RJ, Edwards PR. Analysis of molecular recognition using optical biosensors. Curr Opin Chem Biol 1999;3:544–7.
[4] Liu JW, Lu Y. Adenosine-dependent assembly of aptazyme-functionalised gold nanoparticles and its applications as a colorimetric biosensor. Anal Chem 2004;76:1627–32.
[5] Kogai T, Yoshimura N, Mori T, Yatsuda H. Liquid-phase shear horizontal surface acoustic wave immunosensor. Jpn J Appl Phys 2010;49:07HD15.
[6] Zhoa J, Zhang XY, Yonzon CR, Haes AJ, Van Dayne RP. Localized surface plasmon resonance biosensors. Nanomedicine 2006;1:219–28.
[7] Turner APF. Switching channels makes sense. Nature 1997;387:555–7.
[8] Terrettaz S, Ulrich WP, Vogel H, Hong Q, Dover LG, Lakey JH. Stable self-assembly of a protein engineering scaffold on gold surfaces. Protein Sci 2002;11:1917–25.
[9] Cisneros DA, Muller DJ, Daud SM, Lakey JH. An approach to prepare membrane proteins for single-molecule imaging. Angew Chem Int Ed 2006;45:3252–6.
[10] Shah DS, Thomas MB, Philips S, Cisneros DA, Le Brun AP, Holt SA, et al. Self-assembling layers created by membrane proteins on gold. Biochem Soc Trans 2007;35:522–6.
[11] Foster TJ. Immune evasion by staphylococci. Nat Rev Microbiol 2005;3:948–58.
[12] Uhlén M, Guss B, Nilsson B, Gatenbeck S, Philipson L, Lindberg M. Complete sequence of the staphylococcal gene encoding protein A: a gene evolved through multiple duplications. J Biol Chem 1984;259:1695–702.
[13] Torigoe H, Shimada I, Saito A, Sato M, Arata Y. Sequential ^{1}H NMR assignments and secondary structure of the B domain of staphylococcal protein A: structural changes between the free domain in solution and the Fc-bound B domain in crystal. Biochemistry 1990;29:8787–93.
[14] Deisenhofer J. Crystallographic refinement and atomic models of a human Fc fragment and its complex with fragment B of protein A from *Staphylococcus aureus* at 2.9 and 2.8 Å resolution. Biochemistry 1981;20:2361–70.
[15] Forsgren A, Sjöquist J. "Protein A" from *S. aureus* I. Pseudo-immune reaction with human γ-globulin. J Immunol 1966;97:822–7.
[16] Nilsson B, Moks T, Jansson B, Abrahmsén L, Elmblad A, Holmgren E, et al. A synthetic IgG-binding domain based on staphylococcal protein A. Protein Eng 1987;1:107–13.
[17] Pautsch A, Schulz GE. Structure of the outer membrane protein A transmembrane domain. Nat Struct Biol 1998;5:1013–7.
[18] Pautsch A, Schulz GE. High-resolution structure of the OmpA membrane domain. J Mol Biol 2000;298:273–82.
[19] Prime KL, Whitesides GM. Adsorption of proteins onto surfaces containing end-attached oligo(ethylene oxide): a model system using self-assembled monolayers. J Am Chem Soc 1993;115:10714–21.
[20] Holt SA, Lakey JH, Daud SM, Keegan N. Neutron reflectometry of membrane protein assemblies at the solid/liquid interface. Aust J Chem 2005;58:674–7.
[21] Le Brun AP, Holt SA, Shah DS, Majkrzak CF, Lakey JH. Monitoring the assembly of antibody-binding membrane protein arrays using polarised neutron reflection. Euro Biophys J 2008;37:639–45.
[22] Holt SA, Le Brun AP, Majkrzak CF, McGillivray DJ, Heinrich F, Lösche M, et al. An ion-channel-containing model membrane: structural determination by magnetic contrast neutron reflectometry. Soft Matter 2009;5:2576–86.
[23] Chalton DA, Musson JA, Flick-Smith H, Walker N, McGregor A, Lamb HK, et al. Immunogenicity of a *Yersinia pestis* vaccine antigen monomerized by circular permutation. Infect Immun 2006;74:6624–31.
[24] Löwenadler B, Jansson B, Paleus S, Holmgren E, Nilsson E, Moks T, et al. A gene fusion system for generating antibodies against short peptides. Gene 1987;58:87–97.
[25] Cooke MJ, Philips SR, Shah DSH, Athey D, Lakey JH, Przyborski SA. Enhanced cell attachment using a novel cell culture surface presenting functional domains from extracellular matrix proteins. Cytotechnology 2008;56:71–9.
[26] Whitmore L, Wallace BA. DICHROWEB, an online server for protein secondary structure analysis from circular dichroism spectroscopic data. Nucl Acids Res 2004;32:W668–73.
[27] Keegan N, Wright NG, Lakey JH. Circular dichroism spectroscopy of folding in a protein monolayer. Angew Chem Int Ed 2005;44:4801–4.
[28] Jendeberg L, Persson B, Andersson R, Uhlén M, Nilsson B. Kinetic analysis of the interaction between Protein A domain variants and human Fc using plasmon resonance detection. J Mol Rec 1995;8:270–8.
[29] Thomas RK. Neutron reflection from liquid interfaces. Annu Rev Phys Chem 2004;55:391–426.
[30] Majkrzak CF, Berk NF. Inverting neutron reflectivity from layered film structures using polarised beams. Physica B 1999;267:168–74.
[31] Kienzle PA, Doucet M, McGillivray DJ, O'Donovan KV, Berk NF, Majkrzak CF. GA_refl for the simultaneous fitting of reflection data, http://www.ncnr.nist.gov/reflpak; 2000–2006.
[32] Penfold J. Data interpretation in specular neutron reflection. In: Linder P, Zemb T, editors. Neutron, X-ray and light scattering. Amsterdam: Elsevier; 1991. p. 223–36.
[33] Heinrich F, Ng T, Vanderah DJ, Shekhar P, Mihailescu M, Nanda H, et al. A new lipid anchor for sparsely tethered bilayer lipid membranes. Langmuir 2009;25:4219–29.
[34] McGillivray DJ, Valincius G, Heinrich F, Robertson JWF, Vanderah DJ, Febo-Ayala W, et al. Structure of functional *Staphylococcus aureus* alpha--hemolysin channels in tethered bilayer lipid membranes. Biophys J 2009; 96:1547–53.
[35] Arora A, Abildgaard F, Bushweller JH, Tamm LK. Structure of outer membrane protein A transmembrane domain by NMR spectroscopy. Nat Struct Biol 2001;8:334–8.
[36] Tashiro M, Tejero R, Zimmerman DE, Celda B, Nilsson B, Montelione GT. High-resolution solution NMR structure of the Z domain of staphylococcal protein A. J Mol Biol 1997;272:573–90.
[37] Heing M, Frishman D. STRIDE: a web server for secondary structure assignment from known atomic coordinates of proteins. Nucl Acids Res 2004; 32:W500–2.
[38] Stenberg E, Persson B, Roos H, Urbaniczky C. Quantitative determination of surface concentration of protein with surface plasmon resonance using radiolabeled proteins. J Colloid Interface Sci 1991;143:513–26.

[39] Credergren L, Andersson R, Jansson B, Ulhén M, Nilsson B. Mutational analysis of the interaction between staphylococcal protein A and human IgG1. Protein Eng 1993;6:441–8.
[40] Silverton EW, Navia MA, Davies DR. Three-dimensional structure of an intact human immunoglobulin. Proc Natl Acad Sci USA 1977;74:5140–4.
[41] Geux N, Peitsch MC. SWISS-MODEL and Swiss-Pdb Viewer: an environment for comparative modelling. Electrophoresis 1997;18:2714–23.
[42] Buijs J, Lichtenbelt JWT, Norde W, Lyklema J. Adsorption of monoclonal IgGs and their $F(ab')_2$ fragments onto polymeric surfaces. Colloids Surf B Biointerfaces 1995;5:11–23.
[43] Chen S, Liu L, Zhou J, Jiang S. Controlling antibody orientation on charged self-assembled monolayers. Langmuir 2003;19:2859–64.
[44] Xu H, Zhao X, Grant C, Lu JR, Williams DE, Penfold J. Orientation of a monoclonal antibody at the solid/solution interface: a combined study using atomic force microscopy and neutron reflectivity. Langmuir 2006;22:6313–20.
[45] Xu H, Lu JR, Williams DE. Effect of surface packing density of interfacially adsorbed monoclonal antibody on the binding of hormonal antigen human chorionic gonadotrophin. J Phys Chem B 2006;110:1907–14.
[46] Stanley C, Lew AM, Steward MW. The measurement of antibody affinity: a comparison of five techniques utilizing a panel of monoclonal anti-DNP antibodies and the effect of high antibody on the measurement of low affinity antibody. J Immunol Methods 1983;64:119–32.
[47] Dam TK, Torres M, Brewer CF, Casadevall A. Isothermal titration calorimetry reveals differential binding thermodynamics of variable region-identical antibodies differing in constant region for a univalent ligand. J Biol Chem 2008;283:31366–70.
[48] Buijs J, White DD, Norde W. The effect of adsorption on the antigen binding by IgG and its $F(ab')_2$ fragments. Colloids Surf B Biointerfaces 1997;8:239–49.
[49] Xu H, Xiubo Z, Lu JR, Williams DE. Relationship between the structural conformation of monoclonal antibody layers and antigen binding capacity. Biomacromolecules 2007;8:2422–8.
[50] Wang X, Wang Y, Xu H, Shan H, Lu JR. Dynamic adsorption of monoclonal antibody layers on hydrophilic silica surface: a combined study by spectroscopic ellipsometry and AFM. J Colloid Interface Sci 2008;323:18–25.